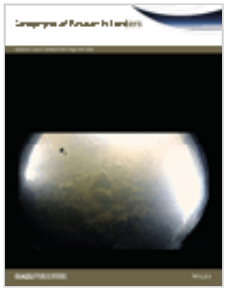

Volume 39, Issue 6

28 March 2012

Brief Detailed

Atmospheric Science

A stochastic parameterization of non-orographic gravity waves: Formalism and impact on the equatorial stratosphere

F. Lott, L. Guez, P. Maury

First Published: 31 March 2012 Vol: 39, L06807 | DOI: 10.1029/2012GL051001

KEY POINTS

- An improved stochastic parameterization of GWs is proposed
- It can be use to help models to simulate the QBO
- It also improves the models to reproduce large-scale equatorial waves

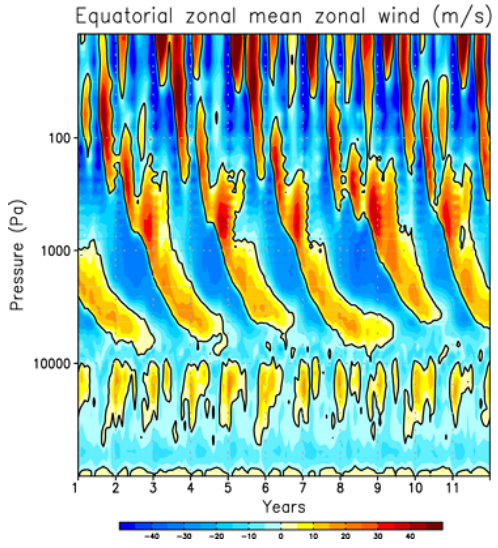

1 of 2

Applying stochastic small-scale damage functions to German winter storms

B. F. Prahl, D. Rybski, J. P. Kropp, O. Burghoff, H. Held

First Published: 23 March 2012 Vol: 39, L06806 | DOI: 10.1029/2012GL050961

KEY POINTS

- Power-law damage function for residential storm loss vs. daily max. wind speed
- Regionally varying large power-law exponents in the range of 8-12
- Correlations between parameters enable reduction of local parameters

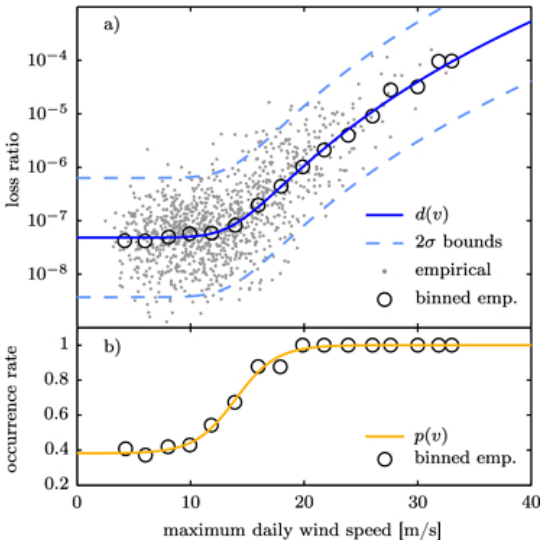

1 of 5

Where is the ideal location for a US East Coast offshore grid?

Michael J. Dvorak, Eric D. Stoutenburg, Cristina L. Archer, Willett Kempton, Mark Z. Jacobson

First Published: 20 March 2012 Vol: 39, L06804 | DOI: 10.1029/2011GL050659

KEY POINTS

- Interconnecting wind sites driven by meso and synoptic scales reduces variability
- Offshore wind farm interconnection reduces variability
- Interconnection benefits can be realized offshore only over distances >450 km

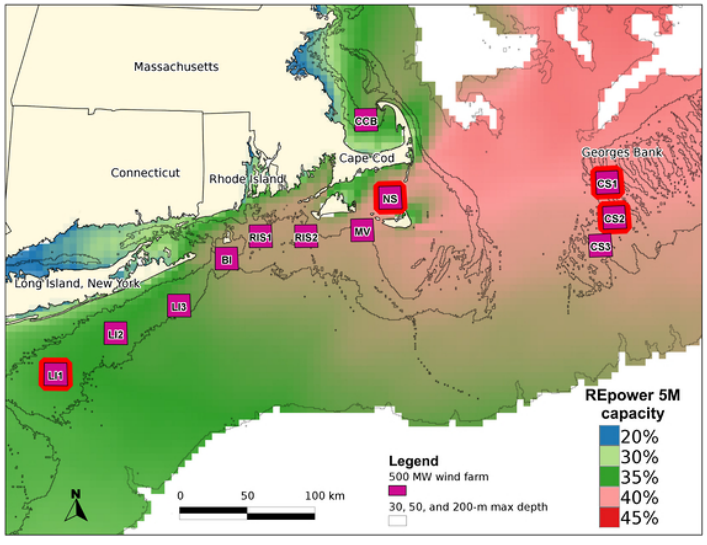

1 of 5

Height-resolved variability of midlatitude tropospheric water vapor measured by an airborne lidar

Lucas Fischer, Christoph Kiemle, George C. Craig

First Published: 20 March 2012 Vol: 39, L06803 | DOI: 10.1029/2011GL050621

KEY POINTS

- Airborne lidar water vapor measurements show power law scaling from 10 to 100 km
- Two-dimensional cross sections show properties depending on height level
- Levels influenced by convection have shallower slopes, higher intermittency

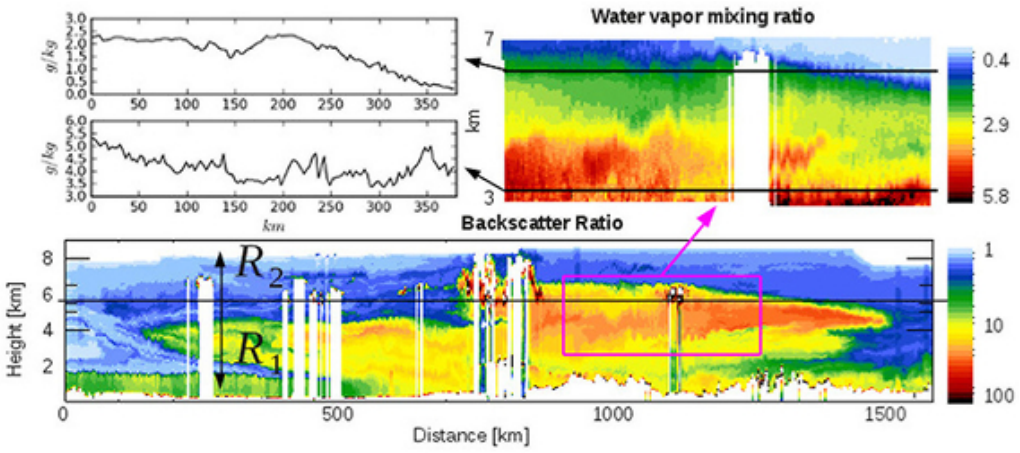

1 of 2

Gasoline emissions dominate over diesel in formation of secondary organic aerosol mass

R. Bahreini, A. M. Middlebrook, J. A. de Gouw, C. Warneke, M. Trainer, C. A. Brock, H. Stark, S. S. Brown, W. P. Dube, J. B. Gilman, et al

First Published: 20 March 2012 Vol: 39, L06805 | DOI: 10.1029/2011GL050718

KEY POINTS

- Diesel emissions contribute significantly to primary organic aerosol
- Gasoline exhaust emissions dominate secondary organic aerosol (SOA) formation
- Globally, SOA from gasoline exhaust may reach 16% of biogenic SOA

Highlight

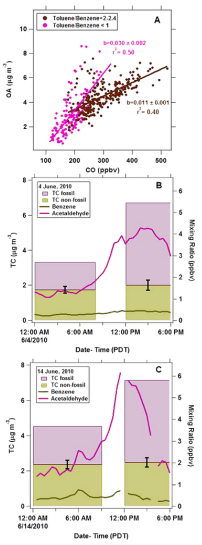

1 of 3

Determination of and evidence for non-core-shell structure of particles containing black carbon using the Single-Particle Soot Photometer (SP2)

Arthur J. Sedlacek III, Ernie R. Lewis, Lawrence Kleinman, Jianzhong Xu, Qi Zhang

First Published: 17 March 2012 Vol: 39, L06802 | DOI: 10.1029/2012GL050905

KEY POINTS

- Analysis technique developed for determination of near-surface black carbon
- A large fraction of BC-containing particles may exist with BC near the surface
- Near-surface BC particles may be associated with biomass burning

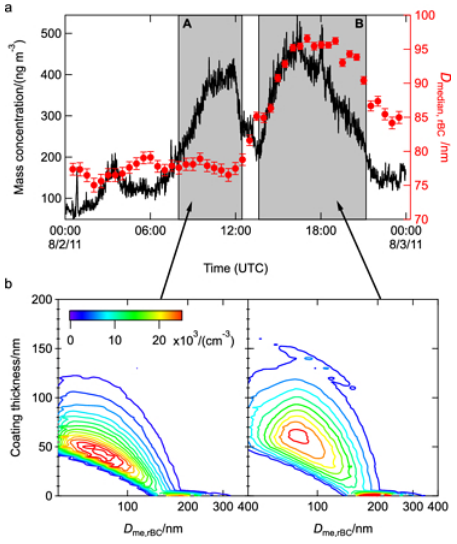

1 of 5

Evidence linking Arctic amplification to extreme weather in mid-latitudes

Jennifer A. Francis, Stephen J. Vavrus

First Published: 17 March 2012 Vol: 39, L06801 | DOI: 10.1029/2012GL051000

KEY POINTS

- Enhanced Arctic warming reduces poleward temperature gradient
- Weaker gradient affects waves in upper-level flow in two observable ways
- Both effects slow weather patterns, favoring extreme weather

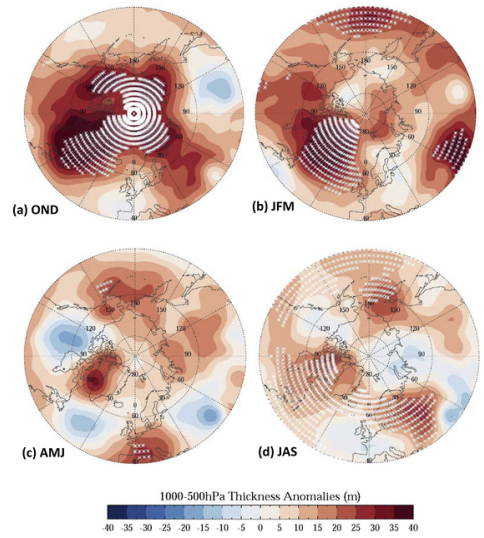

1 of 4

Climate

Nonstationarities of regional climate model biases in European seasonal mean temperature and precipitation sums

D. Maraun

First Published: 28 March 2012 Vol: 39, L06706 | DOI: 10.1029/2012GL051210

KEY POINTS

- Bias correction in general improves future climate simulations
- Cloud cover, soil moisture and albedo changes may cause temperature bias changes
- Precipitation biases in arid regions are affected by internal variability

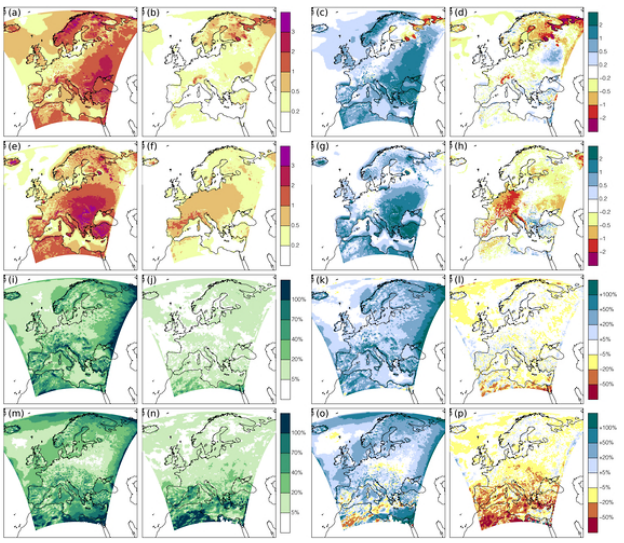

1 of 3

Holocene subsurface temperature variability in the eastern Antarctic continental margin

Jung-Hyun Kim, Xavier Crosta, Veronica Willmott, Hans Renssen, Jérôme Bonnin, Peer Helmke, Stefan Schouten, Jaap S. Sinninghe Damsté

First Published: 28 March 2012 Vol: 39, L06705 | DOI: 10.1029/2012GL051157

KEY POINTS

- Applying a newly developed archaeal membrane lipid-based paleothermometer
- High subsurface temperature variability during the late Holocene
- Variability of Modified Circumpolar Deep Water intrusion into the continental shelf

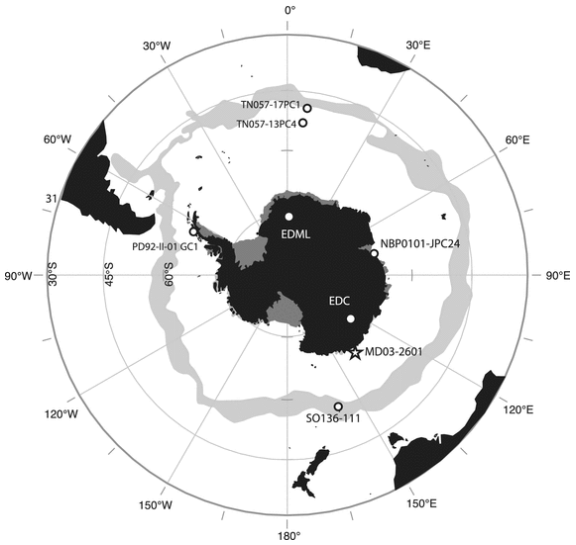

1 of 3

Is a bipolar seesaw consistent with observed Antarctic climate variability and trends?

David P. Schneider, David C. Noone

First Published: 23 March 2012 Vol: 39, L06704 | DOI: 10.1029/2011GL050826

KEY POINTS

- A spurious bipolar seesaw arises from sparse data, especially in the Antarctic
- Caution is advised in analyzing gridded data for Antarctic climate studies
- Regional differences in Antarctic trends partly reflect tropical influences

Highlight

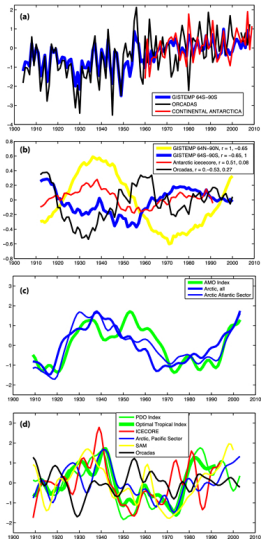

1 of 2

Comparative performance of paleoclimate field and index reconstructions derived from climate proxies and noise-only predictors

Eugene R. Wahl, Jason E. Smerdon

First Published: 20 March 2012 Vol: 39, L06703 | DOI: 10.1029/2012GL051086

KEY POINTS

- Climate proxy data generate high quality reconstructions of temperature fields
- A probabilistic ensemble approach allows clear identification of proxy efficacy

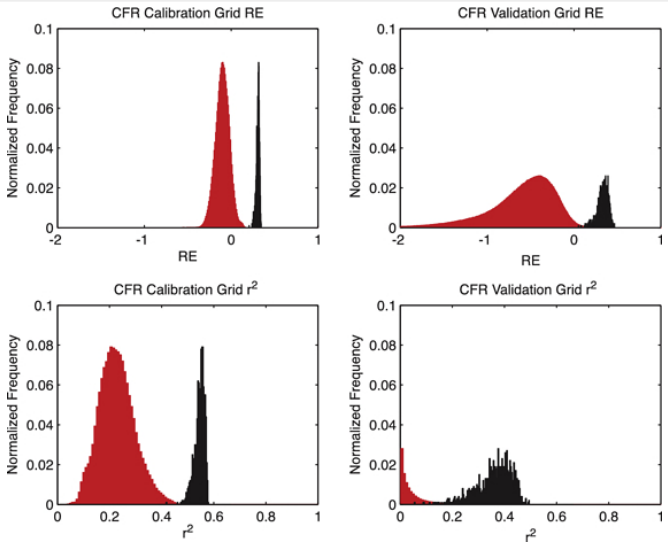

1 of 3

Biomarkers challenge early Miocene loess and inferred Asian desertification

Tingjiang Peng, Jijun Li, Chunhui Song, Zhijun Zhao, Jun Zhang, Zhengchuang Hui, John W. King

First Published: 17 March 2012 Vol: 39, L06702 | DOI: 10.1029/2012GL050934

KEY POINTS

- Tianshui sediments show the ubiquitous presence of middle-chain n-alkanes
- Different patterns between Tianshui sediments and Quaternary loess were observed
- Early Miocene onset of Asian interior desertification needs reevaluate

Highlight

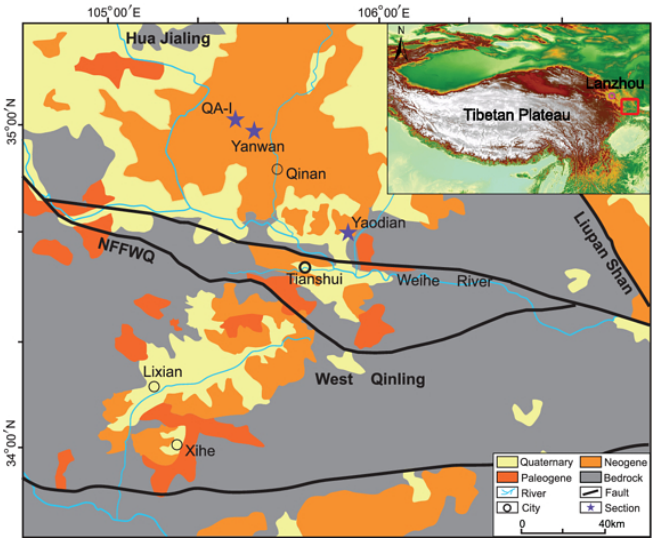

1 of 3

Increase of global monsoon area and precipitation under global warming: A

robust signal?

Pang-chi Hsu, Tim Li, Jing-Jia Luo, Hiroyuki Murakami, Akio Kitoh, Ming Zhao

First Published: 16 March 2012 Vol: 39, L06701 | DOI: 10.1029/2012GL051037

KEY POINTS

- The increase of global monsoon area, precipitation and intensity is robust
- Those changes are consistent with CMIP3 and CMIP5 model projections
- Moisture convergence and evaporation contribute to enhanced monsoon rainfall

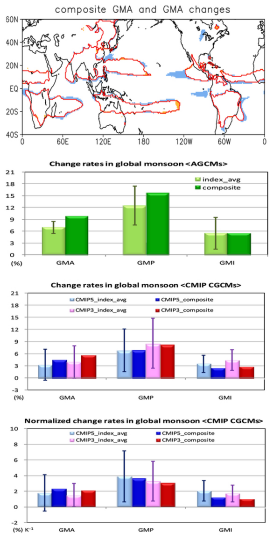

1 of 3

Hydrology and Land Surface Studies

Gross ecosystem photosynthesis causes a diurnal pattern in methane emission from rice

Jaclyn A. Hatala, Matteo Detto, Dennis D. Baldocchi

First Published: 30 March 2012 Vol: 39, L06409 | DOI: 10.1029/2012GL051303

KEY POINTS

- Gross ecosystem photosynthesis drives a diurnal pattern in rice methane flux
- Fluctuations in soil temperature cannot explain the diurnal pattern
- Close photosynthesis-methanogenesis coupling presides the entire rice season

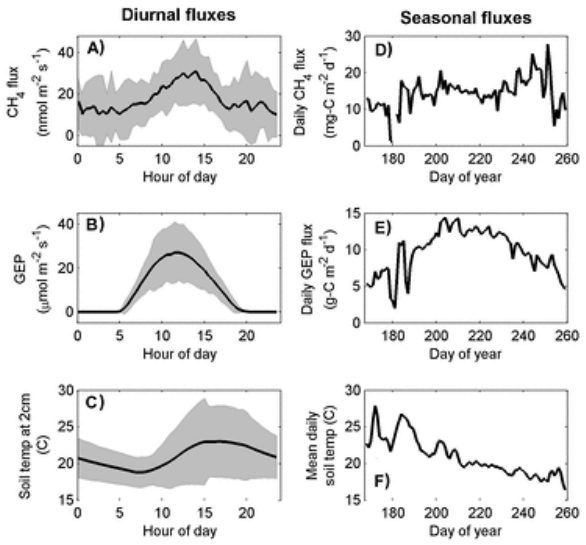

1 of 3

A theoretical framework for the morphodynamics of bedrock channels

Peter A. Nelson, Giovanni Seminara

First Published: 29 March 2012 Vol: 39, L06408 | DOI: 10.1029/2011GL050806

KEY POINTS

- Existing morphodynamic theory requires sufficient sediment supply everywhere
- We extend morphodynamic theory to address problems in bedrock channels
- Sediment cover in bedrock channels tends to become spatially concentrated

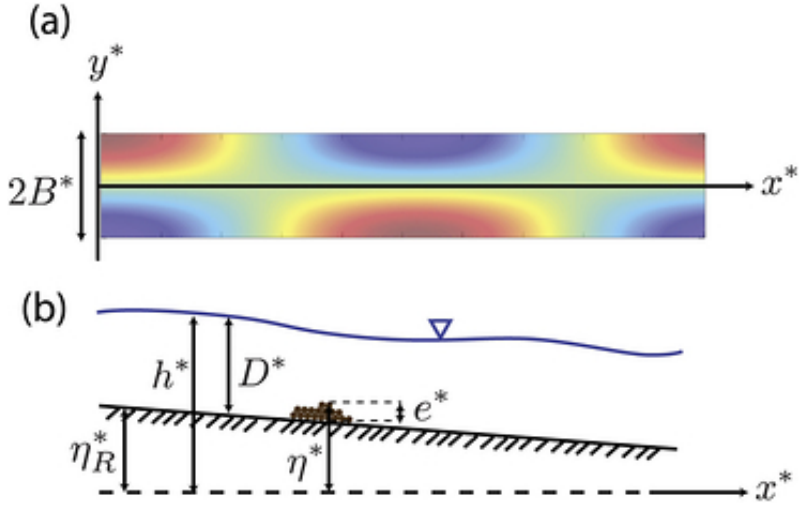

1 of 3

Spontaneous formation and degradation of pool-riffle morphology and sediment sorting using a simple fractional transport model

Gustavo Adolfo Mazza de Almeida, José F. Rodríguez

First Published: 28 March 2012 Vol: 39, L06407 | DOI: 10.1029/2012GL051059

KEY POINTS

- Stream width variations play a key role in the formation of pools and riffles
- The characteristic pool-riffle bed sorting cannot be achieved with steady flows
- Flow-sediment-bed spatio-temporal interactions reinforce pool-riffle structure

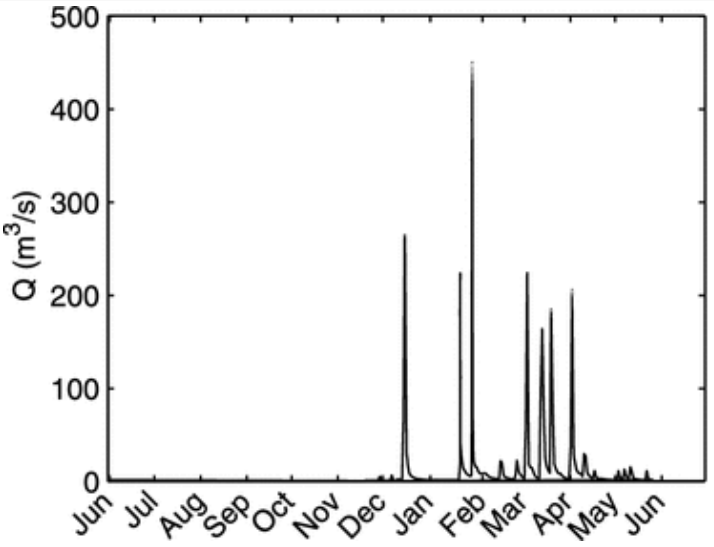

1 of 4

Hillslope asymmetry maps reveal widespread, multi-scale organization

Michael J. Poulos, Jennifer L. Pierce, Alejandro N. Flores, Shawn G. Benner

First Published: 24 March 2012 Vol: 39, L06406 | DOI: 10.1029/2012GL051283

KEY POINTS

- Hillslope asymmetry is mappable at local to global scales
- Hillslope asymmetry is widespread, and varies at multiple scales
- Asymmetry maps facilitate comparison with variations in environmental drivers

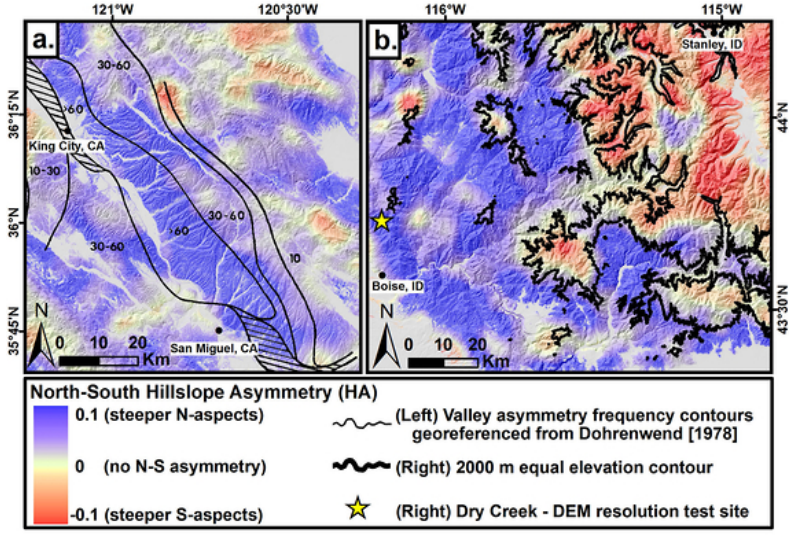

1 of 3

Vertical propagation of lakewide internal waves

Stephen M. Henderson, Bridget R. Deemer

First Published: 23 March 2012 Vol: 39, L06405 | DOI: 10.1029/2011GL050534

KEY POINTS

- In a small lake, observed seiche-like waves propagated vertically
- Drag coefficient model predicted wave absorption in bottom boundary layer
- Theoretically, propagation is favored in short, deep, strongly-stratified lakes

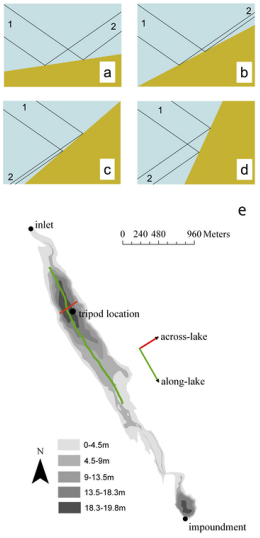

1 of 3

On the temporal variability of the virtual water network

Joel A. Carr, Paolo D'Odorico, Francesco Laio, Luca Ridolfi

First Published: 22 March 2012 Vol: 39, L06404 | DOI: 10.1029/2012GL051247

KEY POINTS

- The network has become more homogeneous but most of the flow is in few links/hub
- 6–8% of the global population controls >50% of the net virtual water exports
- The network is extremely dynamic and intermittent with few permanent links

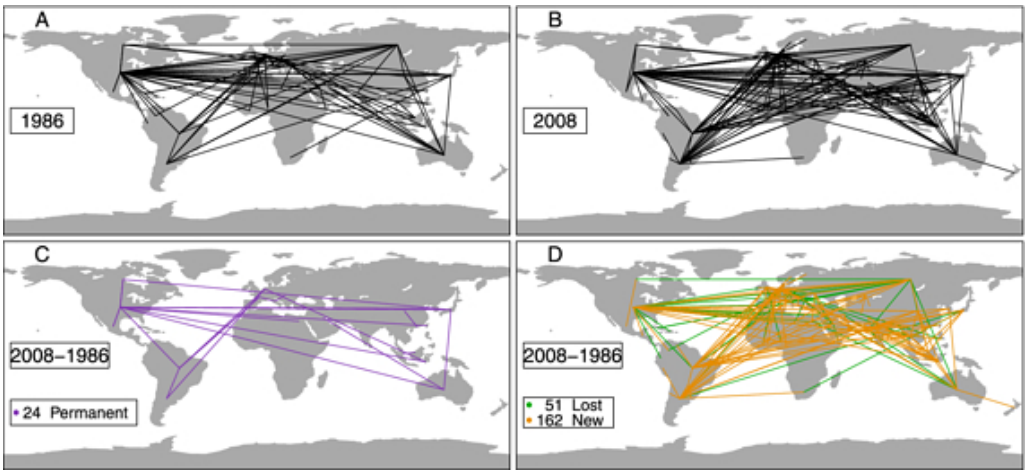

1 of 4

21st century runoff sensitivities of major global river basins

Qiuhong Tang, Dennis P. Lettenmaier

First Published: 21 March 2012 Vol: 39, L06403 | DOI: 10.1029/2011GL050834

KEY POINTS

- Large river runoff sensitivity to global warming is independent of emissions pathway
- Runoff sensitivity to global warming is slightly larger for small temperature changes
- Runoff sensitivity to local forcing changes is generally consistent with observations

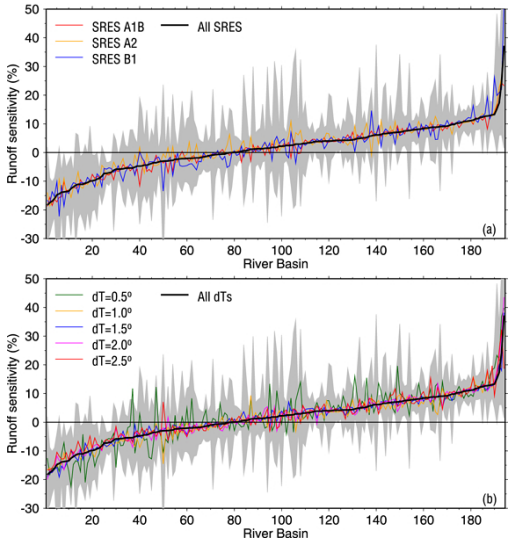

1 of 3

Velocity-dependent capillary pressure in theory for variably-saturated liquid infiltration into porous media

Markus Hilpert

First Published: 21 March 2012 Vol: 39, L06402 | DOI: 10.1029/2012GL051114

KEY POINTS

- Theory for two-phase flow accounts for velocity-dependent capillary pressure
- Saturation overshoot can be described as function of initial liquid content
- The hydrostatic pressure distribution is correctly predicted

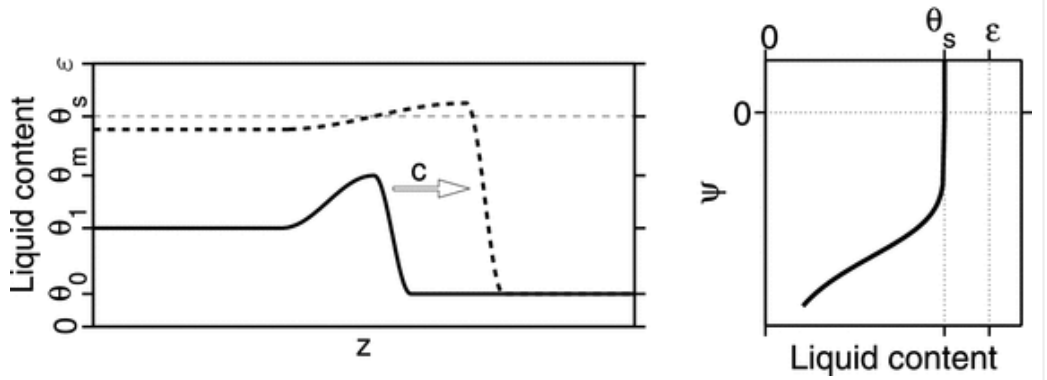

1 of 4

Spatially variable stage-driven groundwater-surface water interaction inferred from time-frequency analysis of distributed temperature sensing data

Kisa Mwakanyamale, Lee Slater, Frederick Day-Lewis, Mehrez Elwaseif, Carole Johnson

First Published: 20 March 2012 Vol: 39, L06401 | DOI: 10.1029/2011GL050824

KEY POINTS

- Time-frequency analysis provides information on strength of groundwater exchange
- S-transform analysis proved a robust indicator of groundwater discharge zones
- Correlation coefficient proved an unreliable indicator of groundwater discharge

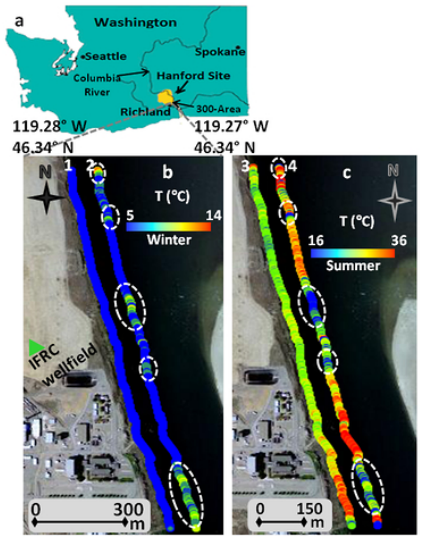

1 of 4

Oceans

On nitrogen fixation and preferential remineralization of phosphorus

F. M. Monteiro, M. J. Follows

First Published: 30 March 2012 Vol: 39, L06607 | DOI: 10.1029/2012GL050897

KEY POINTS

- Differential remineralization may explain observed subsurface maximum of N*
- It may also account for observed temporal variability of N*
- N*-geochemical methods could underestimate marine nitrogen fixation rates

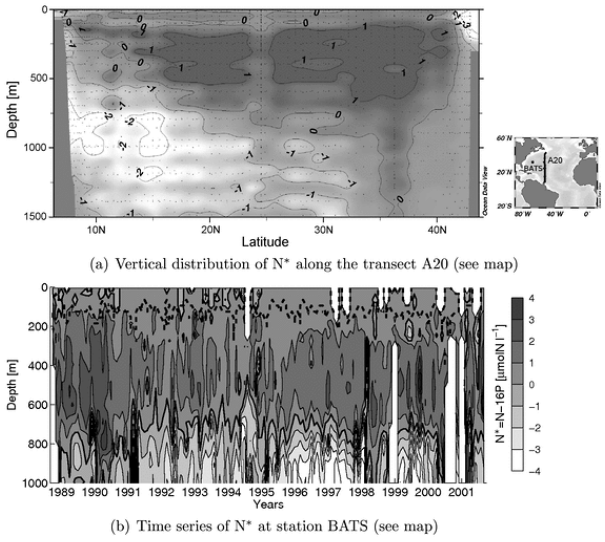

(a) Vertical distribution of N* along the transect A20 (see map)

(b) Time series of N* at station BATS (see map)

1 of 3

Detection and projection of carbonate dissolution in the water column and deep-sea sediments due to ocean acidification

Tatiana Ilyina, Richard E. Zeebe

First Published: 30 March 2012 Vol: 39, L06606 | DOI: 10.1029/2012GL051272

KEY POINTS

- Carbonate dissolution has low potential to mitigate ocean acidification
- Calcite undersaturation extending up to 100 m after 2100
- Detectable dissolution-driven changes projected after 2070 in the surface ocean

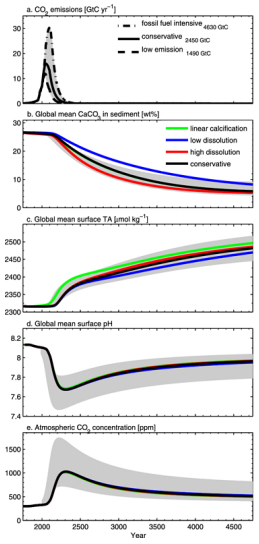

1 of 3

Summer thermal structure and anticyclonic circulation of Lake Erie

Dmitry Beletsky, Nathan Hawley, Yerubandi R. Rao, Henry A. Vanderploeg, Raisa Beletsky, David J. Schwab, Steven A. Ruberg

First Published: 29 March 2012 Vol: 39, L06605 | DOI: 10.1029/2012GL051002

KEY POINTS

- Currents measured in the central basin were anticyclonic
- Bowl-shaped thermocline is linked to Ekman pumping

Highlight

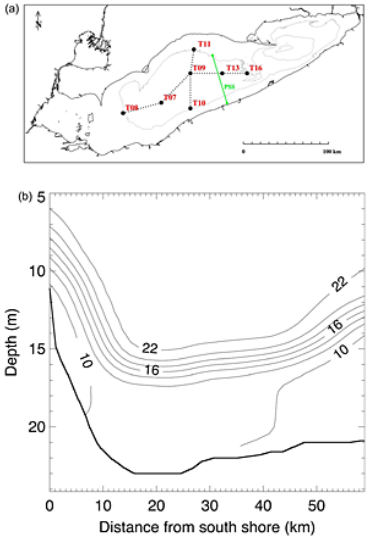

1 of 3

Linkages among interannual variations of shoreline, wave and climate at Hasaki, Japan

Y. Kuriyama, M. Banno, T. Suzuki

First Published: 27 March 2012 Vol: 39, L06604 | DOI: 10.1029/2011GL050704

KEY POINTS

- Interannual shoreline variation was induced by wave fluctuation
- 45% of the shoreline variation was attributable to large-scale climate variation

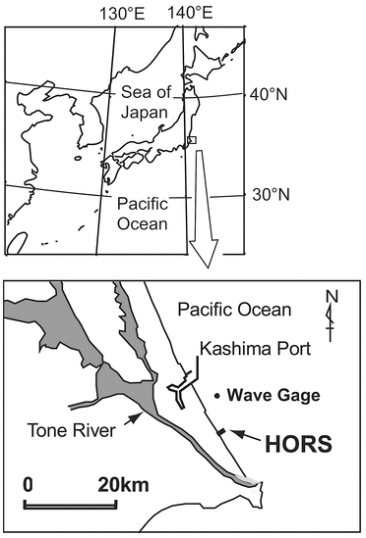

1 of 3

On the impact of wind forcing on the seasonal variability of Weddell Sea Bottom Water transport

Q. Wang, S. Danilov, E. Fahrbach, J. Schröter, T. Jung

First Published: 27 March 2012 Vol: 39, L06603 | DOI: 10.1029/2012GL051198

KEY POINTS

- Answer how wind forcing influences the shelf water export
- Answer how important is the gyre circulation for WSBW transport
- Unstructured models are useful for answering questions linking different scales

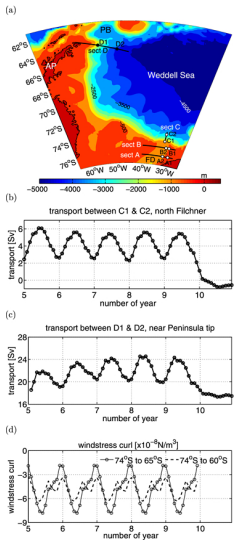

1 of 4

The impact of advective transport by the South Indian Ocean Countercurrent on the Madagascar plankton bloom

F. Huhn, A. von Kameke, V. Pérez-Muñuzuri, M. J. Olascoaga, F. J. Beron-Vera

First Published: 24 March 2012 Vol: 39, L06602 | DOI: 10.1029/2012GL051246

KEY POINTS

- SICC largely controls Madagascar plankton bloom
- SICC provides eastward transport and meridional confinement
- Bloom's origin probably located at south tip of Madagascar

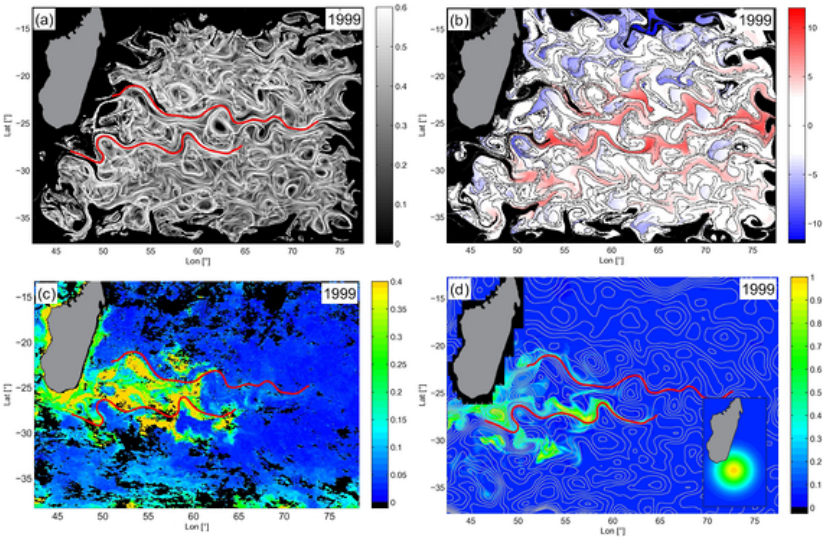

1 of 3

Tasman leakage in a fine-resolution ocean model

Erik van Sebille, Matthew H. England, Jan D. Zika, Bernadette M. Sloyan

First Published: 24 March 2012 Vol: 39, L06601 | DOI: 10.1029/2012GL051004

KEY POINTS

- In the OFES model, Tasman leakage is on average 4.2 Sv, 30% of ITF flux
- Tasman leakage heat flux is between 0.08 and 0.18 PW, which is not insignificant
- Less then half of Tasman leakage is within eddies, which affects monitoring

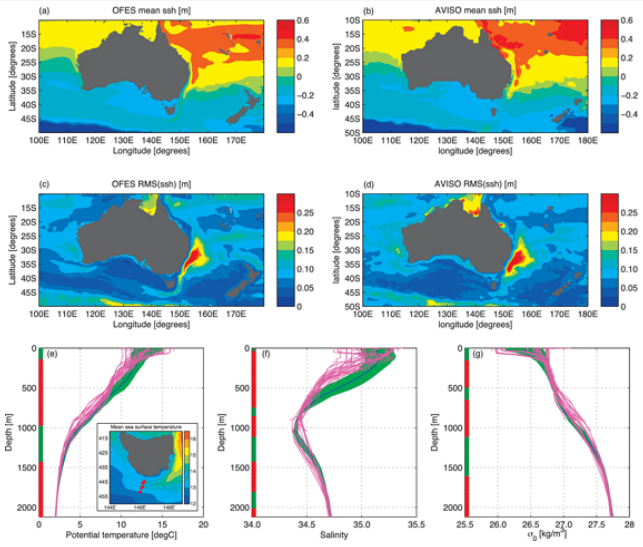

1 of 3

Solid Earth

Recent geodetic unrest at Santorini Caldera, Greece

Andrew V. Newman, Stathis Stiros, Lujia Feng, Panos Psimoulis, Fanis Moschas, Vasso Saltogianni, Yan Jiang, Costas Papazachos, Dimitris Panagiotopoulos, Eleni Karagianni, et al

First Published: 30 March 2012 Vol: 39, L06309 | DOI: 10.1029/2012GL051286

KEY POINTS

- Santorini is deforming appreciably for the 1st time since its last eruption
- A dense GPS network has unprecedented data coverage
- Activity is centered in the region that blew-out in the 1650 BC Minoan Eruption

Highlight

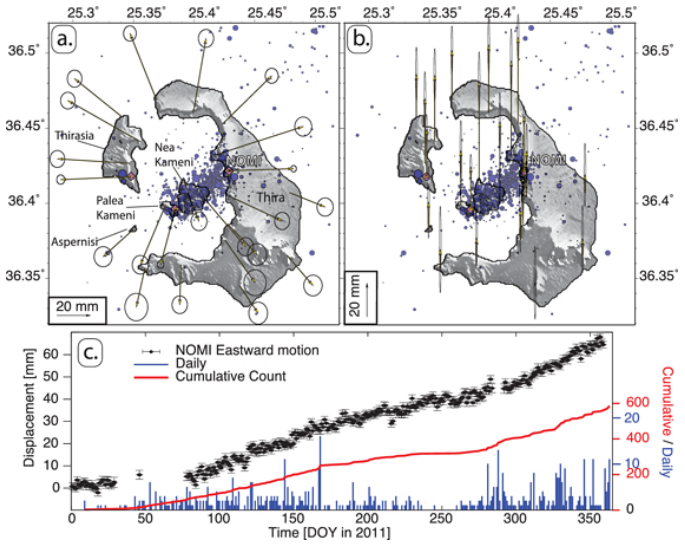

1 of 4

Are megaquakes clustered?

Eric G. Daub, Eli Ben-Naim, Robert A. Guyer, Paul A. Johnson

First Published: 29 March 2012 Vol: 39, L06308 | DOI: 10.1029/2012GL051465

KEY POINTS

- Large earthquakes do not cluster in time
- Below M=7.3, earthquakes are clustered, though possibly due to data uncertainty
- Transparent statistical measures can be used to study earthquake clustering

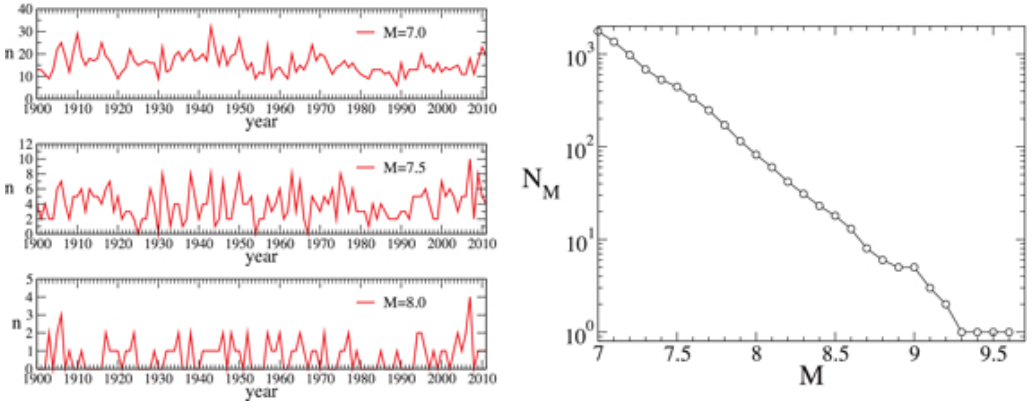

1 of 5

A year of lava fountaining at Etna: Volumes from SEVIRI

G. Ganci, A. J. L. Harris, C. Del Negro, Y. Guehenneux, A. Cappello, P. Labazuy, S Calvari, M. Gouhier

First Published: 28 March 2012 Vol: 39, L06305 | DOI: 10.1029/2012GL051026

KEY POINTS

- Characterisation of radiant heat flux curves for Etna's 2011-12 lava fountains
- A new cooling model to yield magnitude and intensity of fountaining events
- Consistency of annual DRE volume and mean TADR with Etna's recent eruptive activity

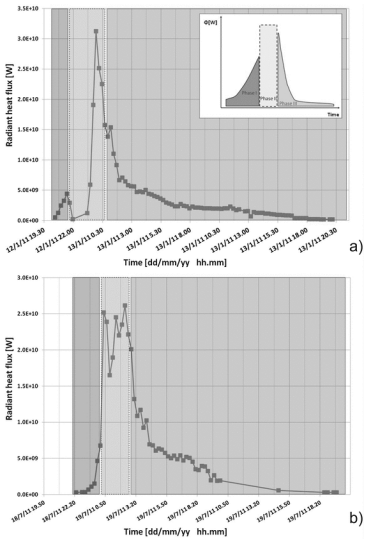

1 of 3

First volatile inventory for Gorely volcano, Kamchatka

A. Aiuppa, G. Giudice, M. Liuzzo, G. Tamburello, P. Allard, S. Calabrese, I. Chaplygin, A. J. S. McGonigle, Y. Taran

First Published: 28 March 2012 Vol: 39, L06307 | DOI: 10.1029/2012GL051177

KEY POINTS

- First gas inventory for Gorelyi volcano; refinement of Kamchatka gas budget
- Assessment of volatile abundances and origins in NW Pacific mantle source
- New constraints on volatile recycling at destructive (arc) plate margins

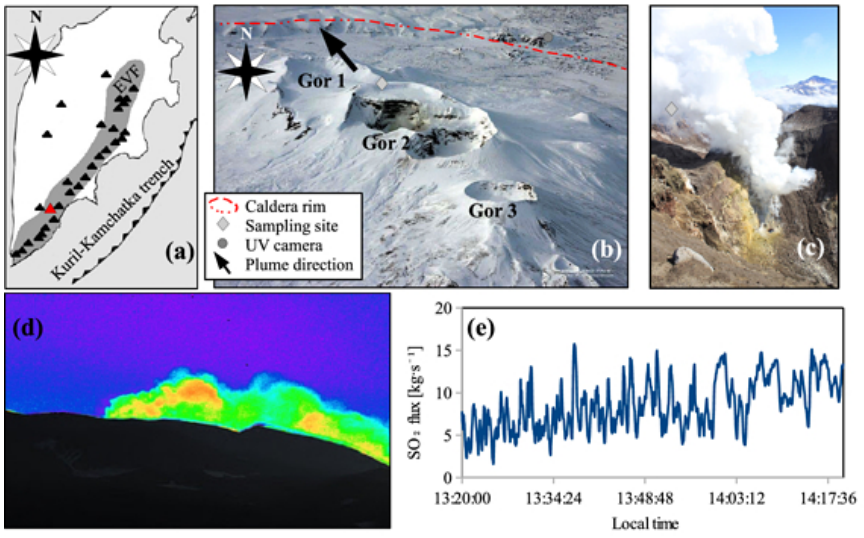

1 of 4

Influence of hydrogen on the electronic states of olivine: Implications for electrical conductivity

Duojun Wang, Shun-ichiro Karato, Zaiyang Liu

First Published: 28 March 2012 Vol: 39, L06306 | DOI: 10.1029/2012GL051046

KEY POINTS

- Dissolution of hydrogen in olivine modifies its electronic structure
- Charged hydrogen-related species increase number of electron holes
- Increased number of electron holes enhances electrical conductivity and creep

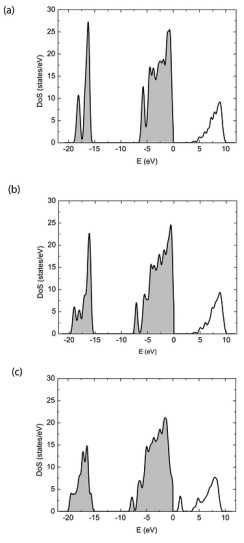

1 of 4

Evidence of a partitioned dynamo reversal process from paleomagnetic recordings in Tahitian lavas

Kenneth A. Hoffman, Nobutatsu Mochizuki

First Published: 27 March 2012 Vol: 39, L06303 | DOI: 10.1029/2011GL050830

KEY POINTS

- Axial dipole and flux in the shallow core reverse quasi-independently
- Two-stage geodynamo reversal process, possibly due to stratification
- Supports contention of a long-held influence over pattern by lower-most mantle

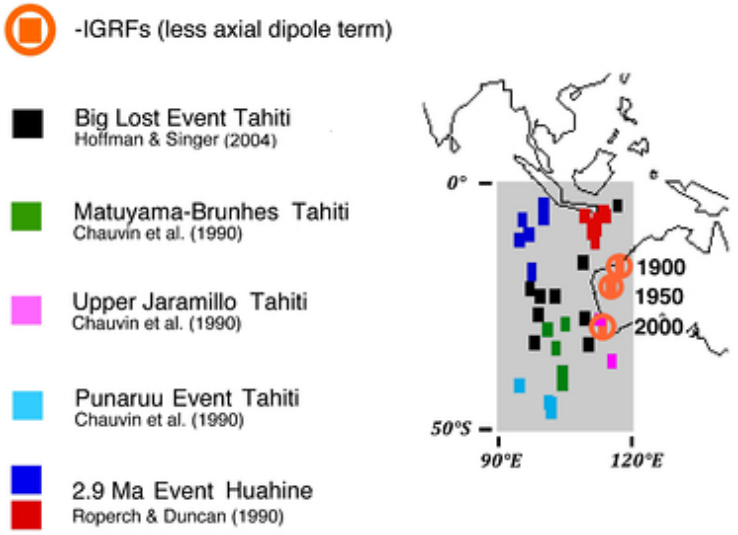

1 of 5

Elasticity of phase D and implication for the degree of hydration of deep subducted slabs

Angelika D. Rosa, Carmen Sanchez-Valle, Sujoy Ghosh

First Published: 27 March 2012 Vol: 39, L06304 | DOI: 10.1029/2012GL050927

KEY POINTS

- Elasticity of phase D, a water carrier in cold suducted slabs
- Plausible candidate to explain low velocity zones and shear splitting in Tonga
- Implications for the degree of hydration of the deep subducted slab

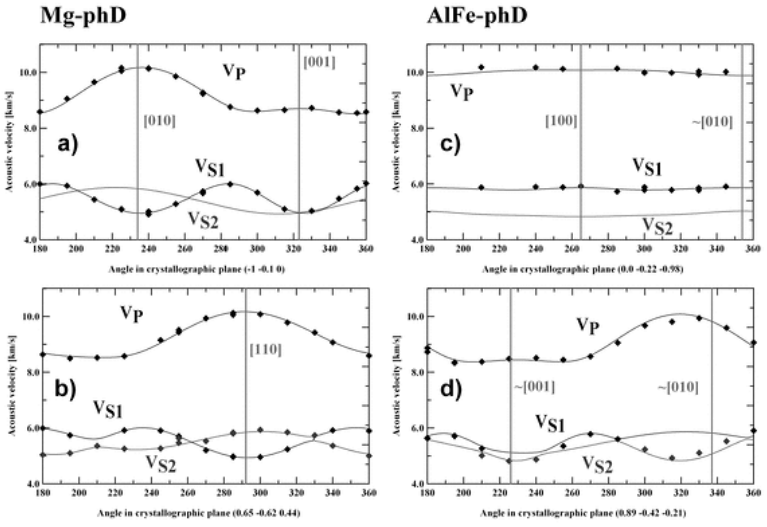

1 of 2

On the reported ionospheric precursor of the 1999 Hector Mine, California earthquake

J. N. Thomas, J. J. Love, A. Komjathy, O. P. Verkhoglyadova, M. Butala, N. Rivera

First Published: 24 March 2012 Vol: 39, L06302 | DOI: 10.1029/2012GL051022

KEY POINTS

- The essential results of Pulinets et al. (2007) are reproduced
- Anomalous signal is part of normal global-scale TEC variation
- The method of Pulinets at al. could not have been used for prediction

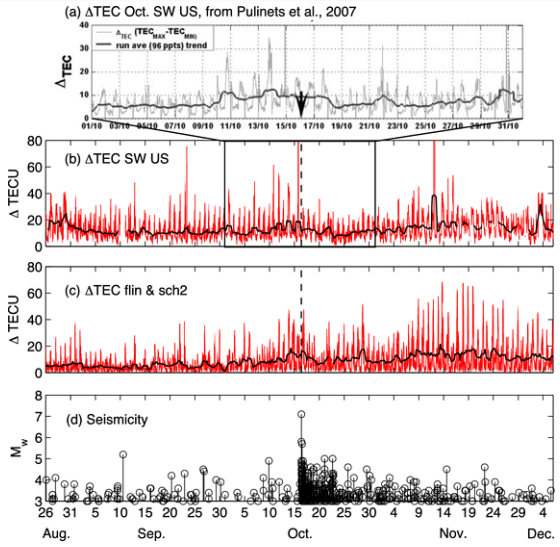

1 of 2

Ambient-field Green's functions from asynchronous seismic observations

Shuo Ma, Gregory C. Beroza

First Published: 17 March 2012 Vol: 39, L06301 | DOI: 10.1029/2011GL050755

KEY POINTS

- The coda of amibent-noise Green's functions is stable over time
- It is possible to extract Green's functions from data recorded asynchronously
- A new mode for observational seismology is suggested

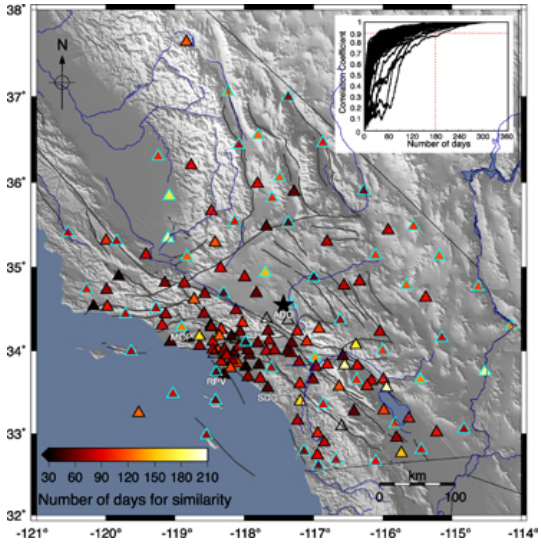

1 of 5

Space Sciences

Sudden intensity increases and radial gradient changes of cosmic ray MeV electrons and protons observed at Voyager 1 beyond 111 AU in the heliosheath

W. R. Webber, F. B. McDonald, A. C. Cummings, E. C. Stone, B. Heikkila, N. Lal

First Published: 29 March 2012 Vol: 39, L06107 | DOI: 10.1029/2012GL051171

KEY POINTS

- Structure in the outer heliosheath and the proximity to the heliopause
- Galactic electron intensity increases and the overall heliospheric modulation
- Periodic 13-27 day variations and their relation to the wavy current sheet

Highlight

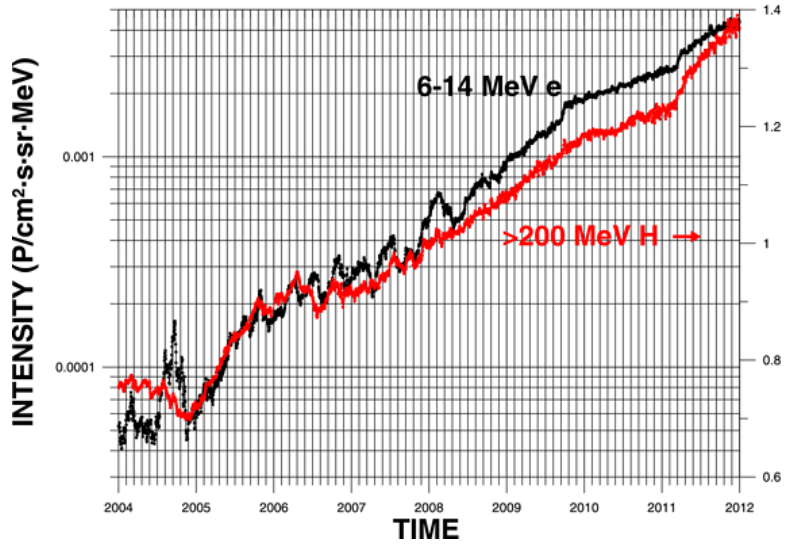

1 of 2

Spacecraft charging near Enceladus

H.-W. Hsu, M. Horányi, S. Kempf, E. Grün

First Published: 29 March 2012 Vol: 39, L06108 | DOI: 10.1029/2012GL050999

KEY POINTS

- Two dust currents are introduced for the spacecraft charging calculation
- The spacecraft potential is neutralized by the dust currents
- Dust impact plasma may affect in-situ thermal plasma measurements

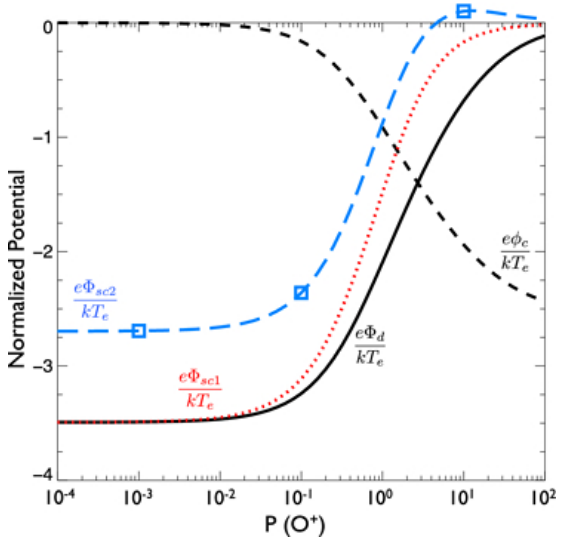

1 of 2

Plasma pressure generated auroral current system: A case study

S. B. Mende, S. L. England, H. U. Frey

First Published: 28 March 2012 Vol: 39, L06106 | DOI: 10.1029/2012GL051211

KEY POINTS

- Describes how pressure gradients produce auroral currents
- In a case study shows that the currents are large enough to create auroras
- Shows that closed magnetic field lines must be stretched for aurora generation

Open Access

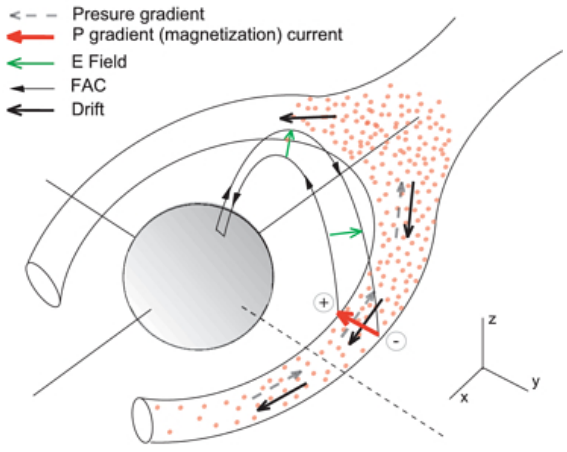

1 of 4

Electric structure of dipolarization front at sub-proton scale

H. S. Fu, Y. V. Khotyaintsev, A. Vaivads, M. André, S. Y. Huang

First Published: 27 March 2012 Vol: 39, L06105 | DOI: 10.1029/2012GL051274

KEY POINTS

- We calculate E at DF using single- and four- spacecraft methods
- Normal E is balanced by the Hall (dominant) and pressure gradient terms
- At dawn flank, E is dawnward; At dusk flank, E is duskward

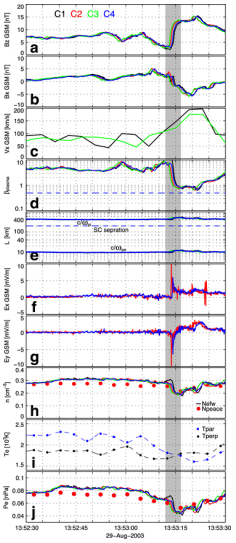

1 of 4

Kelvin-Helmholtz stability of reconnection exhausts in the solar wind

Y. L. Sasunov, V. S. Semenov, M. F. Heyn, I. V. Kubyshkin, H. K. Biernat

First Published: 24 March 2012 Vol: 39, L06104 | DOI: 10.1029/2012GL051273

KEY POINTS

- Tangential discontinuities as boundaries of solar wind exhaust regions
- Riemannian decay of a current sheet due to reconnection
- Kelvin-Helmholtz analysis of solar wind exhaust boundaries

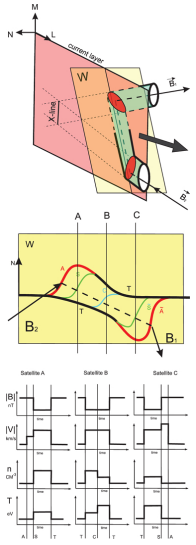

1 of 4

Statistical modeling of plasmaspheric hiss amplitude using solar wind measurements and geomagnetic indices

D. I. Golden, M. Spasojevic, W. Li, Y. Nishimura

First Published: 23 March 2012 Vol: 39, L06103 | DOI: 10.1029/2012GL051185

KEY POINTS

- A model of hiss amplitude vs. L and MLT is described
- This model is more accurate than a model which uses only AE* as input
- Evolution of plasmaspheric hiss amplitude as a function of storm phase is shown

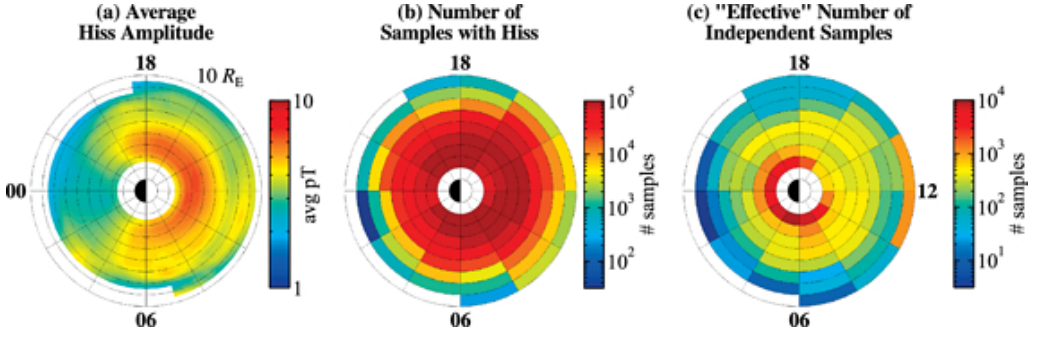

1 of 3

Effects of amplitude modulation on nonlinear interactions between electrons and chorus waves

X. Tao, J. Bortnik, R. M. Thorne, J. M. Albert, W. Li

First Published: 22 March 2012 Vol: 39, L06102 | DOI: 10.1029/2012GL051202

KEY POINTS

- A method is shown to model realistic chorus packets
- Chorus subpackets can affect nonlinear electron-chorus interactions
- The subpackets should be included in modeling the electron-chorus interactions

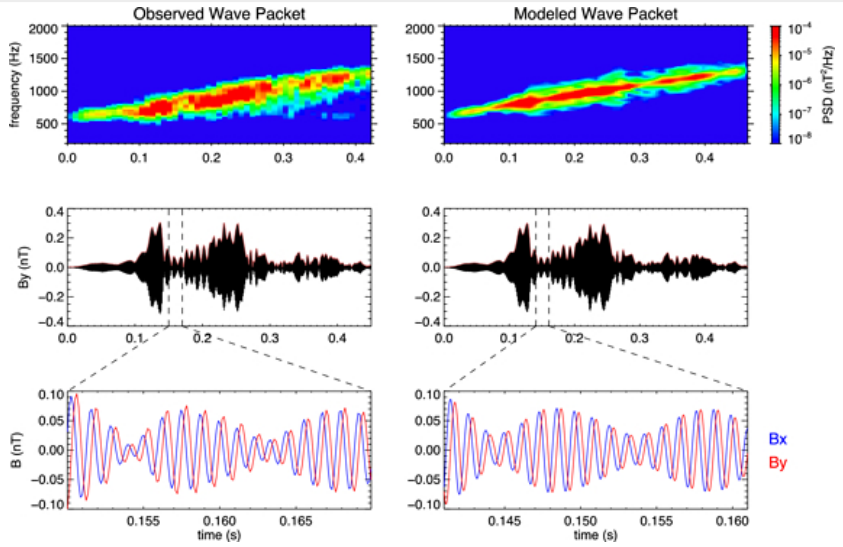

1 of 3

Solar flare impacts on ionospheric electrodyamics

Liying Qian, Alan G. Burns, Stanley C. Solomon, Phillip C. Chamberlin

First Published: 20 March 2012 Vol: 39, L06101 | DOI: 10.1029/2012GL051102

KEY POINTS

- Flares have significant impacts on ionosphere electrodynamics
- Upward ExB drifts initially weaken causing weakening of the Appleton anomaly
- Upward ExB drifts strengthen for extended time causing extended TEC disturbance

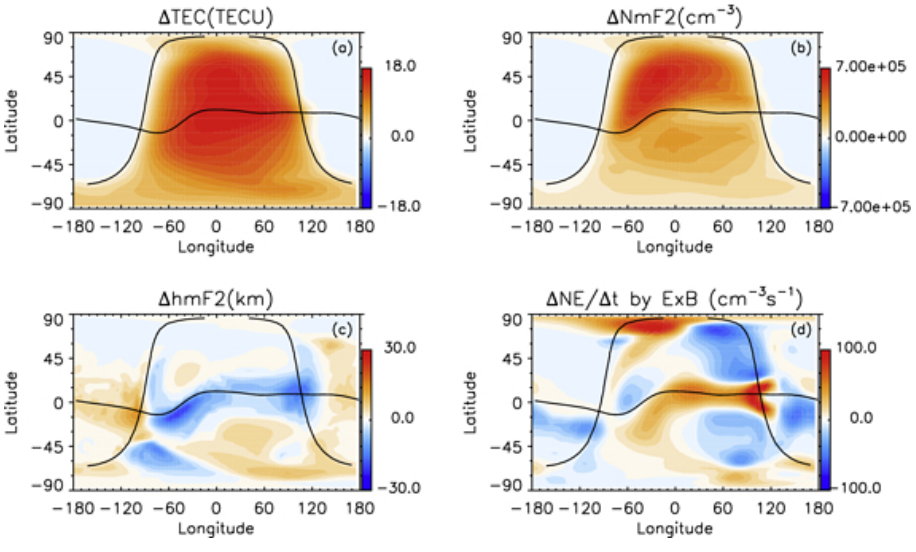

1 of 4

The Cryosphere

Regions of rapid sea ice change: An inter-hemispheric seasonal comparison

Sharon Stammerjohn, Robert Massom, David Rind, Douglas Martinson

First Published: 16 March 2012 Vol: 39, L06501 | DOI: 10.1029/2012GL050874

KEY POINTS

- In some regions the ice-free season has increased by >3 months over the last 32 years
- Anomalies in sea ice retreat & subsequent advance show strong correspondence
- Results support a positive atmospheric-ocean-ice feedback over summer but not winter

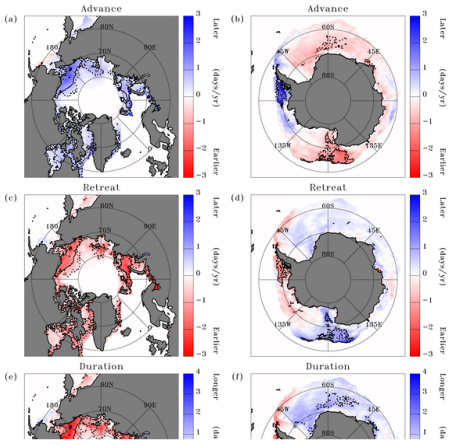

1 of 3

Current Issue

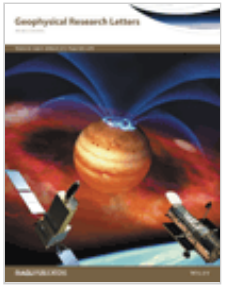

Volume 42
Issue 6
28 March 2015

All Issues
Browse a free sample issue

Find an article

and

or

Stay Connected to Eos

Access Eos Archive Issues

Issues from 1997-2014 are freely available to the public.

Older issues are available through AGU membership or through an institutional subscription.

Journal Resources

Call for Papers

Special Section Proposal Form

Personal Choice

Terms of Use

Cover Gallery

Institutional Subscription Rates

Get RSS Feed

Featured Special Collection

The Early Results from the Van Allen Probes

NASA's Van Allen Probes mission is designed to acquire data to solve key questions about the energetics and dynamics of the Earth's Van Allen Radiation belts that have arisen from active research in the domain in the past decades.

Editors' Highlights

- **What Causes Sunspot Pairs?**
- **Water Beneath the Surface of Mars, Bound up in Sulfates**
- **When Predicting Drought Risk, Do Not Overlook Temperature**
- **Changing Patterns in U.S. Air Quality**

See all »

Download the app

Download the Geophysical Research Letters app on your iPad

Upcoming AGU Meetings

Triennial Earth-Sun Summit

26 Apr - 1 May 2015
Indianapolis, Indiana, USA

2015 Joint Assembly

3-7 May 2015
Montreal, Canada

Chapman Conference on Evolution of the Asian Monsoon and its Impact on Landscape, Environment and Society: Using the Past as the Key to the Future

14-19 June 2015
Hong Kong SAR, China

See all »